

Air-Blast and the Science of Dynamic Pressure Measurements

Patrick L. Walter, PCB Piezotronics, Depew, New York and Texas Christian University Fort Worth, Texas

Considering current world events, the accurate measurement of the dynamic pressure associated with air-blast, as well as its effect on structures, is highly important. Yet, the accurate measurement of this pressure remains one of the biggest challenges that can be presented to the measurement engineer. This article attempts to provide guidance to enhance the quality of these measurements. In order to provide this guidance, a large body of the science of dynamic pressure measurement has been both summarized and organized. It is hoped that this work will also serve as a reference for other activities where the measurement of dynamic pressure has importance.

An explosion in air is a process by which a rapid release of energy generates a pressure wave of finite amplitude. The energy source can be anything that generates a violent reaction when initiated. This includes: chemical or nuclear materials, gases (high pressure gas-storage vessels, steam boilers), or electricity (spark gap, rapid vaporization of a metal). The properties of air will cause the front of this pressure wave to “shock up” or steepen as the front moves. The result is a shock front moving supersonically, i.e., faster than the sound speed of the air ahead of it, with discontinuities in pressure, density, and particle velocity across the front.

Unlike acoustic waves that move at sonic velocity, produce no finite change in particle velocity, and don’t “shock up,” air-blast is a nonlinear process involving nonlinear equations of motion. Air-blast can be encountered in freely expanding shocks in air or, if obstacles enclose the energy source, in directed shocks and contained shocks. Examples of all three are shown in Figure 1.

A near-ideal explosion that is generated by a spherically symmetric source, and that occurs in a still, homogeneous atmosphere, would result in a pressure-time history similar to the one illustrated in Figure 2. The pressure is at ambient until the air-blast arrives. At this time it instantaneously rises to its peak side-on overpressure, decays back to ambient, drops to a partial vacuum, and eventually returns to ambient.

Deviations from this ideal waveform are to be expected. Rarefaction waves occur at the contact surface between the explosion products and air; these waves result in modification of the positive shock phase.

For caged explosives, any fragment that is generated may have an associated momentum adequate for it to outrun the blast-wave velocity and produce disturbances before the wave’s arrival. Ground effects due to dust or heat-reflecting surfaces may form a precursor wave.

Additionally, if the blast wave has low specific energy, it may travel a significant distance before “shocking up.” The interaction of blast waves with a solid object can result in reflections from the object or cause the waves to reflect from as well as diffract around the object.

Figure 3 shows the reflection of strong shock waves from a reflective surface. I_1 , I_2 , and I_3 represent the expanding shock wave, while the R contours represent the respective reflections from the surface. When I_1 just touches the surface S , a reflection occurs that is more than two times I_1 . As the shock wave continues to move outward, the intersection of each I and its corresponding R lies on the dashed line. The incident and reflected shocks coalesce to form a Mach stem. As the shock expands, the Mach stem grows, eventually encompassing the 2-shock system above it.

As the blast wave propagates to greater distances from its source, its magnitude lessens and it decreases in velocity un-

til it propagates at the speed of sound. Theoretically, acoustical laws could then apply, but meteorological conditions tend to control its properties at long distances.

The development of predictive codes and analytical techniques for the strength and directional characteristics of blast-waves is highly dependent on experimental measurements. Robust blast-pressure transducers were not always available to make these measurements; they had to be developed.

Much of the early development of these blast-pressure transducers occurred at government laboratories such as the Ballistic Research Laboratory (BRL – United States) and Royal Armament Research and Development Establishment (RARDE – United Kingdom) in the 1950s and 1960s. Among the early commercial pressure transducer developers were Atlantic Research Corporation, Kaman Nuclear Corporation, Kistler Instrument Corporation (where some of its founders subsequently formed PCB Piezotronics), and Shaevitz-Bytrex Corporation.

To characterize the time signature of a blast-pressure event, transducers are required for two types of measurements. Side-on transducers (incident) are those that record free field pressure at varying distances from the blast source. Their design must minimize interference with the flow behind the shock front. Reflected-pressure transducers are used for measuring pressures reflected at normal or oblique incidence from a rigid surface. Flow and diffraction effects are no longer important. This type of transducer must be mounted so that its sensing surface is flush with the reflecting surface for the shock front.

One of the notable pioneers in this field was Mr. Ben Granath who originally worked at BRL and subsequently founded Susquehanna Instruments, a development company for blast transducers. This company is now a part of PCB Piezotronics. Photographs of two transducers, which resulted from Mr. Granath’s work, are provided as Figure 4.

In Figure 4A, the pencil probe, is obviously intended for side-on pressures. Its quartz acceleration compensated piezoelectric sensing element is built into the housing. The geometry of the contained piezoelectric element, as well as the velocity of the shock front of the blast wave passing over it, control its rise time. This transducer covers a pressure range extending to 1000 psi. The transducer in Figure 4B works on the principle of a pressure bar. Its sensing element is tourmaline, which is interfaced to an internal bar. The bar is acoustically impedance-matched to the tourmaline, resulting in a 1.5-MHz resonant frequency for the transducer. This model transducer is used for reflected pressure measurements to 20,000 psi.

A limitation of the early piezoelectric transducers developed by government labs and/or industry was the influence of the cable on their signal. In hazardous tests, such as those involving explosives, cable lengths of hundreds to thousands of feet are typical. When these cable lengths were employed with charge-sensing circuits, a variety of deleterious effects would result; the principal problems were:

- Noise generated within the cable due to triboelectric effects.
- The high cost of special noise-treated cables to eliminate the above effects.
- A charge sensing amplifier’s noise level, which increases in proportion to cable capacitance, i.e., cable length.

All of the aforementioned problems have subsequently been solved with integral-electronics piezoelectric (IEPE) transducers. PCB Piezotronic’s equivalent registered trademark, which predates the IEPE designator, is ‘ICP®.’ The IEPE configuration converts the transducer’s output to low impedance, thus eliminating triboelectric effects, and it also permits the use of a va-



Figure 1. Examples of freely expanding (A), directed (B), and contained air-blasts (C).

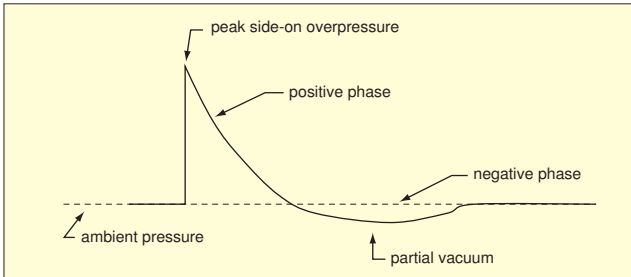


Figure 2. Ideal side-on pressure record attributable to a spherical symmetric source in a homogeneous medium.

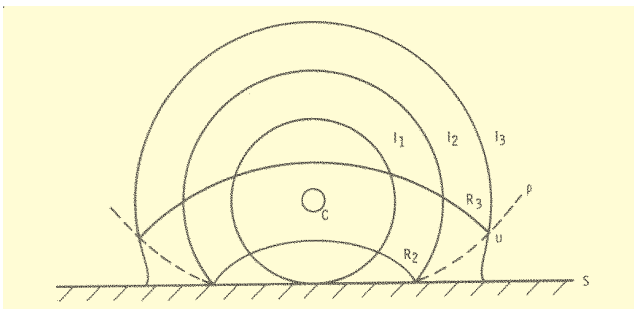


Figure 3. Strong shock wave interaction with a reflective surface.

riety of inexpensive 2-wire cable systems, none of which require noise treatment. In addition, if a typical 20-milliamp current is used to power the transducer, the high-frequency response of the transducer is maintained over very long cable runs. Figure 5 shows a cross-sectional view of a vibration compensated pressure transducer in an IEPE or ICP® configuration.

Interfacing the Blast Pressure Transducer

Of initial concern in the application of modern transducers to measure air-blast phenomena is the interface between the blast pressure transducer and the measurand (the blast environment). Figure 4 showed a Model 137A ICP® blast pressure transducer in a pencil probe configuration for side-on pressure measurements. In application, its axis must be aligned incident (perpendicular) to the incoming air blast wave. Its size should be small relative to the highest frequency of interest in the shock front. For example, assume a shock front is moving at 3,300 feet per second. The wavelength λ corresponding to a spectral frequency f of 20,000 Hz in the front would be:

$$\lambda f = c = 3300 \text{ (12) inches per second or}$$

$$\lambda = 1.98 \text{ inches.}$$

Looking at the dimensions of the pencil probe in Figure 6 relative to the preceding value of λ , it is clear that the probe has the potential to act as a reflecting body to high frequencies in the approaching shock front.

In order to minimize reflections, the probe is tapered over approximately its first two-inches of length. It then transitions into a cylindrical body with a flat surface on one side. This flat surface eliminates discontinuities between an embedded, disc-shaped, radial facing, quartz sensing element and the transducer housing. Ideally, the velocity of the shock front and the spatial averaging of the disc as the front traverses across it will control the measured rise time. The averaging effect associated with any pressure transducer can be envisioned as the distur-



Figure 4: PCB blast pressure transducers.

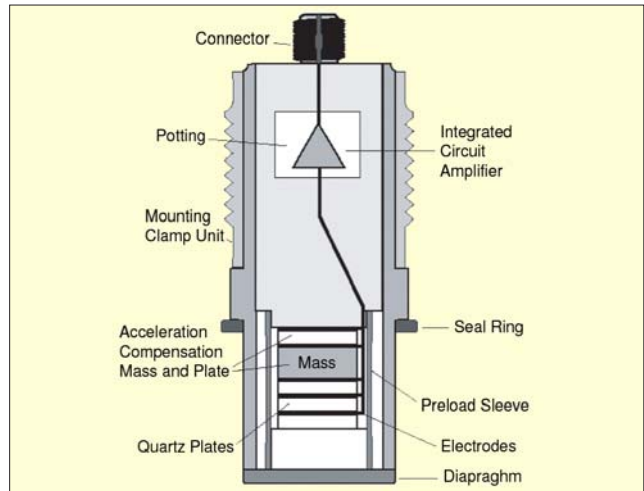


Figure 5. ICP® vibration compensated pressure transducer.

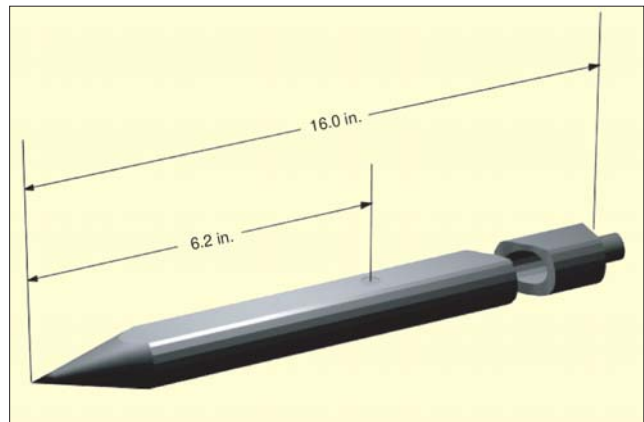


Figure 6. Outline drawing of the Pencil Probe in Figure 4.

tion that a sine wave would encounter as it passes at right angles to the axis of symmetry that is perpendicular to the plane of the circular diaphragm of the transducer. The diaphragm would cause distortion through spatial averaging of the wave, which results in attenuation.

Analysis of the spatial averaging effect of the diaphragm of pressure transducers has been performed.¹ Results are shown in Figure 7. When using these results, the velocity (in/second) of the gas passing over the transducer must be applied as a multiplier to the abscissa (x-axis) to convert its units to Hz. As an example of the application of Figure 7, at 1100 ft/sec (13,200 in/sec) in dry air, a 0.3-in. diameter diaphragm would nominally produce a five-percent amplitude error at 9,200 Hz, and a 0.1-in. diameter diaphragm would produce the same error at 24,000 Hz.

For reflected pressures at a stationary barrier, the averaging effects due to flow at normal incidence are not a consideration. However, the diaphragm of the transducer should be flush with the reflecting surface. If the diaphragm is flush, the structural properties of its sensing element control its dynamic performance. However, in some instances, deviations from flush mounting might be required.

These deviations could be needed to isolate the transducer from high temperature or some other harsh environment. In this situation, the transducer could be coupled to the process by a length of tubing or other intermediate fitting. The resultant

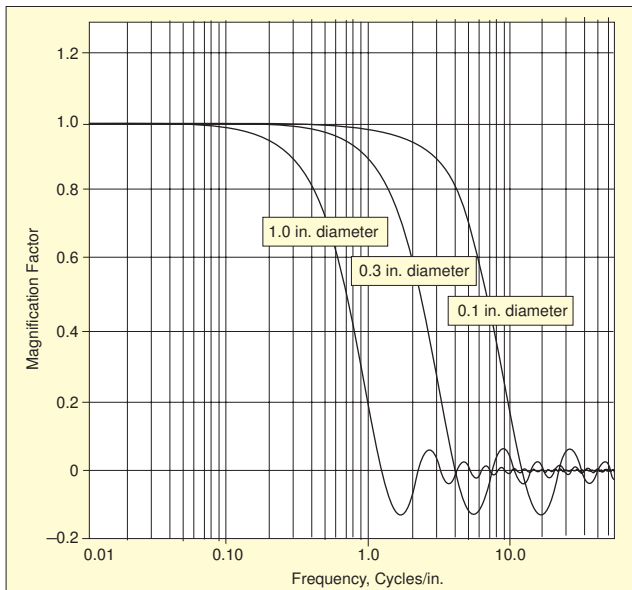


Figure 7. Frequency response of spatial averaging pressure transducers

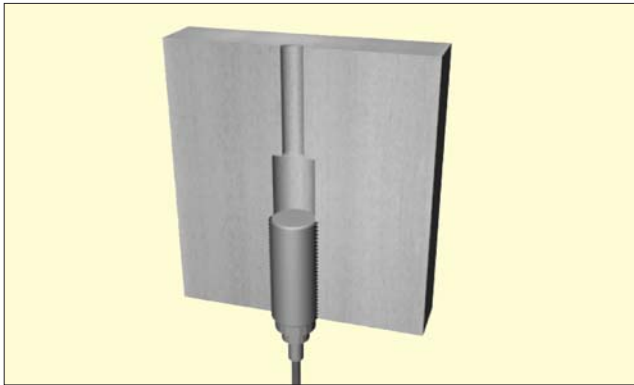


Figure 8. Pressure transducer with tubing and associated volume interconnect.

passageway could even be filled with a porous material of high specific heat capacity to further reduce the temperature of the gaseous explosion products, thus lessening their effect on transducer performance. However, this recess mounting of the transducer severely degrades its ability to measure the initial reflected blast pressures accurately. On occasion, this compromise may be justified in an attempt to quantify the total pressure impulse, which requires a longer measurement time, or, in the case of an enclosed explosive, the residual contained pressure in the enclosure after the blast occurs.

Acoustic theory, while not exact, provides us with guidance to estimate this degradation in transducer performance. In Figure 8 we see a transducer mounted with an associated volume in front of its sensing face. A long cavity or equivalent tube provides the interconnection to this volume. Based on the assumption that all dimensions are much less than the wavelength of sound at the frequency at which this system is designed to operate, an analysis of this cavity as a second order single-degree-of-freedom system can be performed. For a short tube, the Helmholtz resonator model² yields a natural frequency in Hz of:

$$f_n = \frac{c \sqrt{\frac{\pi d^2}{4V(L + 0.85d)}}}{4\pi} \quad (1)$$

In this equation, c is the velocity of sound of the gas being measured (≈ 1100 ft/sec for room-temperature air), V is the volume of the lower cavity, L is the length of the entrance tube, and d is the diameter of this tube.

If the entrance tube in Figure 8 is lengthened to cause the

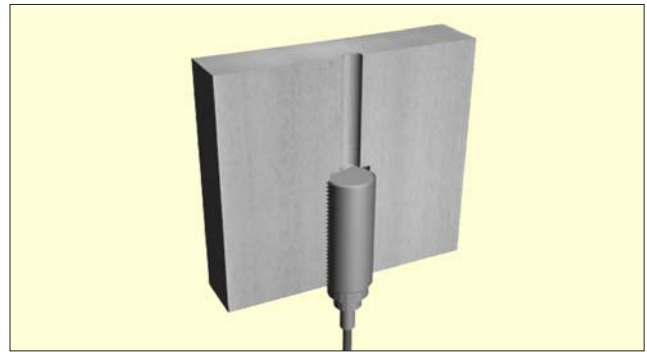


Figure 9. Pressure transducer with tubing interconnect.

lower volume V to become less significant relative to the volume of the tube (Figure 9), and if the tube is sufficiently narrow that the displacement of the gas at any instant is the same at all points on its cross section, it can be modeled by the wave equation.² Results are:

$$f = \frac{c(2n-1)}{4L} \quad (2)$$

where $n = 1$ corresponds to the first natural frequency; c and L have the same meaning as before. It's been suggested that the Helmholtz resonator model (equation #1) should transition to the wave equation model (equation #2) when the volume of the tube is about one-half the volume of the chamber.

It is interesting to make a representative calculation using one of these equations. Assume that a pressure transducer with a resonant frequency of 100 kHz is mounted at the end of a standpipe of length 1.5 in. measuring reflected blast pressures at 500° Fahrenheit (F). The sound velocity in air is proportional to the square root of the absolute temperature. Therefore, 1100 ft/sec at room temperature [70° F or 530° R (Rankine)] would scale to $\sqrt{960}/\sqrt{530}$ or about 1480 ft/sec at 500° F or 960° R. Using Equation (2), the effective resonance of the transducer/tube combination would be lowered from 100 kHz to 2,960 Hz! Equations 1 and 2 then enable calculation of an approximate value as to how much the dynamic response of a pressure transducer is reduced when coupled through a gas-filled cavity.

When performing explosively driven blast pressure measurements, these equations may yield somewhat imprecise results because gas composition and temperature, and thus sound velocity, are often unknown. However, when comparing the speed of sound for gases such as methane, air, and carbon dioxide, it can be concluded that an acceptable starting point for most calculations is to assume air to be the gas in the cavity at a temperature of 500° F.

Data Validation

After the pressure transducer is properly mounted, it is important to consider data validation. In addition to pressure, which is the desired environment to be measured, there are competing undesired environments that occur concurrent with the pressure environment. These include, as a minimum: transient temperature, light, acceleration, strain, ionization products of the detonation, and others. When considering the potential effects of these undesired environments, it can be seen that strain, acceleration and temperature can all interact with the piezoelectric crystal within the transducer to result in an erroneous pressure indication. In addition, thermoelectric, photoelectric, electromagnetic, triboelectric, and other energy induced effects can result in additive electrical signals that create errors in the transducer output. All of these extraneous signals can be viewed as noise, which contaminates the desired pressure measurement. To validate that the transducer output signal is not contaminated (i.e., it is solely attributable to pressure), a combination of placebo³ and 'check'⁴ channels must be used.

If one looks at the piezoelectric d-coefficients of quartz, they appear as:

$$\begin{aligned}
 P_{xx} &= d_{11}\sigma_{xx} - d_{11}\sigma_{yy} + 0\sigma_{zz} + d_{14}\tau_{yz} + 0\tau_{zx} + 0\tau_{xy} \\
 P_{yy} &= 0\sigma_{xx} + 0\sigma_{yy} + 0\sigma_{zz} + 0\tau_{yz} - d_{14}\tau_{zx} - 2d_{11}\tau_{xy} \\
 P_{zz} &= 0\sigma_{xx} + 0\sigma_{yy} + 0\sigma_{zz} + 0\tau_{yz} + 0\tau_{zx} + 0\tau_{xy}
 \end{aligned}
 \quad (3)$$

These equations show that there is one crystal axis of quartz (z-axis, 3rd equation) that produces no piezoelectric output when stress is applied. Figure 10 contains a boule of quartz with this axis (z) identified. It is possible to manufacture a placebo blast transducer, i.e., one that produces no piezoelectric output, using z-cut quartz.

The placebo transducer can be applied in the test in the same manner as any of the operational transducers, but it will not respond to mechanical inputs (pressure, acceleration, strain). Any electrical output from it identifies signal contamination due to thermoelectric, photoelectric, electromagnetic, and/or triboelectric effects. In reality, a signal from the placebo transducer is typically caused by electrical or magnetic noise induced effects and indicates that the operational transducers are probably also similarly contaminated. Triboelectric (i.e., frictionally generated) charge effects in cables can be ruled out as a noise source if integral electronics (ICP®) are included within or at the transducer. This is because, as noted previously, ICP® converts the transducer to an equivalent low-impedance voltage source. Just as an electrical signal from a placebo transducer indicates signal contamination, no electrical signal from it indicates the effects responsible for the contamination to be absent.

Light intensity should also have no influence on the transducers discussed to date. Thermal effects will subsequently be discussed as a separate topic.

It remains yet to determine whether strain and/or acceleration result in additional contamination of the signal from the pressure transducer. Strain and acceleration have a cause/effect relationship. For example, under pressure induced acceleration loading, flexural modes of vibration might be excited in a plate in which a blast pressure transducer is mounted. The plate's motion elicits an acceleration response from the transducer by inducing stress in the piezoelectric element of the transducer, as does the resultant strain.

To identify the combined effect of acceleration and strain on the piezoelectric element, we take an operational transducer and isolate it from the desired pressure environment. It becomes a 'check' channel. The right-hand portion of Figure 11 shows the field application of a 'check' transducer. An operational transducer is mounted per the manufacturer's specifications in a hole dimensioned deep enough to prevent the transducer from making contact. If necessary, a small weep-hole can be drilled into the hole from the back surface of the plate to assure that no pressure build-up occurs due to flexing under pressure loads of the material in front of the transducer diaphragm. Any signal output from the check channel in excess of that produced by the placebo transducer is noise induced by strain and/or acceleration.

Under no circumstances can the undesired response from either the placebo transducer or 'check' channel be 'subtracted' from the signal of the pressure measuring transducer(s) as a data correction scheme. This is because the undesired environments contained in the pressure transducer(s) signals are spatially distributed across the test item. Thus, phasing errors would occur. The next several paragraphs, up to and including Figure 11, outline the process(es) and analysis that must be undertaken in order to replicate the effect of the 'subtraction' if it could legitimately occur.

The combination of the placebo transducer and the 'check' transducer allows us to document almost all of the aforementioned undesired responses with the noted exception of thermal effects due to transient temperature. The Model 134 Blast Probe (Figure 4) is principally used to define the fast-rise-time shock front. Due to the acoustic wave-guide principle on which the probe operates, a thin layer of black tape on its front face is required to mitigate thermal inputs to its very thin tourmaline crystal. This transducer is not intended to record the en-

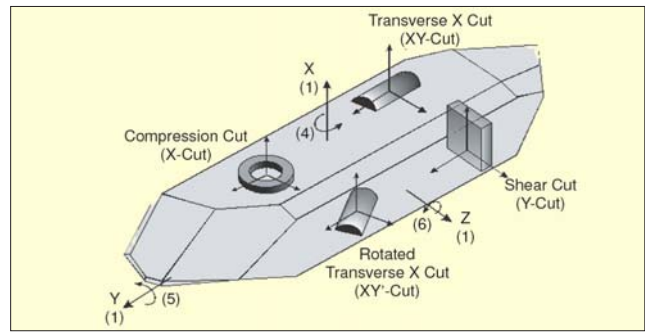


Figure 10. Quartz boule with linear and rotational axes' directions identified.



Figure 11. Strain isolated pressure transducer left – isolated 'check' transducer right.

tire pressure-time history of the blast pulse. Adding additional tape at the probe's front boundary will provide greater thermal delay, but will also result in increased mechanical impedance, which degrades performance. Thus, its application is limited to short record times. Longer record times, such as those required for the total pressure impulse, necessitate a transducer with a mechanical configuration like that shown in Figure 5. Fortunately a transducer made like Figure 5 produces a very recognizable signature when a transient thermal input creates a problem. A thermal transient initially couples into and causes various dimensional changes followed by expansion of the preload sleeve containing the quartz crystal assembly. The byproduct of this later expansion shows up as a positive (i.e., nonreturn to zero) signal residing after the blast event is clearly over.

Every manufacturer's transducers will respond to these undesired environments. However, some respond much less than others. The question is: "How do you manage or mitigate these responses?" Limited examples follow.

Thermal transient responses must be mitigated by application of ceramic or RTV coatings on the face of the transducer diaphragm. These provide a thermal delay, hopefully until the blast event is over. Reference 5 provides one such quantitative study of time delays that are achievable.

Figure 11 (left side) shows how a strain-induced signal can be eliminated as a noise source through mechanical isolation, in this case, via a concentric groove machined around the transducer to interrupt the strain transmission path. Low-density foam can be used to fill this groove to prevent a discontinuity to the flow of the blast products.

Previously, Figure 5 showed how essentially building an accelerometer within the pressure transducer, if its output is added in opposition to the acceleration response of the pressure-sensing element, could minimize acceleration effects. If the acceleration-compensation mass is further adjusted, the sensor's frequency response is also enhanced. This is called "frequency tailoring."

Elimination of those noise-induced signals uniquely identified by the placebo transducer would likely occur through attention to proper grounding and shielding. It should be noted that electrostatic shielding materials (e.g., copper, aluminum)

are very poor electromagnetic shielding materials.

As can be seen, once documented, the various undesired responses require individual noise-reduction solutions. After additional tests in which both the placebo and 'check' transducers produce no output, the pressure signals on the other data channels can be considered validated. That is, all the recorded data can now be considered to be the appropriate response of the pressure transducer(s) to the pressure environment alone.

Getting the Signal Down the Cable

Thus far, we have provided an understanding of the air blast environment and the operation of transducers intended to measure it. We went on to describe how to mount these transducers to optimize their dynamic response and how to validate the resultant signal output from the transducers. These considerations alone don't guarantee success unless we are able to transmit the signal down the cable with fidelity. Since, as mentioned previously, hundreds or thousands of feet of cable can be involved, signal distortion can occur.

For the following discussion, the consideration of a lossless transmission line (one whose resistance is ignored) will suffice. A voltage signal V going down the line is a function of both space (z) and time (t), i.e., $v = v(z,t)$. Its equation can be given as:⁶

$$\frac{\partial^2 v(z,t)}{\partial z^2} = lc \frac{\partial^2 v(z,t)}{\partial t^2} \quad (4)$$

where l and c are the line inductance and capacitance per unit length. This is the classical wave equation that governs many other physical phenomena such as stress wave transmission in a bar and acoustic wave transmission in an organ pipe. By analogy, $1/\sqrt{lc}$ has a dimension of velocity.

Many facilities, where air-blast testing is performed, also measure and record data from strain gages and other bridge type circuits. Therefore, 4-wire shielded cable is typically used. A representative instrumentation cable could be: Belden⁷ non-paired #82418, 4-conductor, 18 AWG, fluorinated ethylene propylene insulation, Beldroid[®] shielded, with an inductance of 0.15 $\mu\text{H}/\text{ft}$ and a conductor-to-conductor capacitance of 30 pF/ft. Using the above equation ($1/\sqrt{lc}$) to calculate the propagation velocity for this cable results in 0.47×10^9 ft/sec or roughly 0.5 the speed of light.

The characteristic impedance for a lossless line is expressed as $\sqrt{l/c}$, which for the preceding cable can be calculated to be 70.7 ohms. If the connecting cable is terminated properly ($\sqrt{l/c} = 70.7$ ohms), there will be no reflections at high frequencies. However, if the cable is not terminated properly (e.g., if it operates directly into a high impedance amplifier (typically $R \geq 1$ M Ω)), reflections can occur. The first reflection will occur at a frequency f corresponding to a wavelength λ equal to four (4) times the cable length.

As an example, arbitrarily pick the highest signal frequency of interest to be 100,000 Hz. The corresponding wavelength is:

$$\lambda f = (4L)f = \text{propagation velocity or} \quad (5)$$

$$\lambda = 4L = \frac{0.47 \times 10^9 \text{ ft/s}}{1 \times 10^5 \text{ Hz}} = 4700 \text{ ft}$$

Thus, a cable length of (4700/4) or 1175 feet will result in oscillations at a frequency of 100,000 Hz. In addition, signal fidelity can only be maintained to approximately 20,000 Hz, which is one-fifth the frequency of oscillation.

Figure 12 shows an obtained, experimental frequency response for 400 ft of a 4-conductor shielded Belden instrumentation cable of #22 AWG. Note the resonant frequency at 330,000 Hz for the infinite load $R = 1$ M Ω . If we calculate the fundamental wavelength for this cable, and again use 0.47×10^9 ft/sec, which is an approximation for this cable, we get $\lambda = 4L = (0.47 \times 10^9 \text{ ft/sec}) / (3.3 \times 10^5 \text{ Hz}) = 1,424$ ft or a cable length of $1,424/4 = 356$ ft, which agrees reasonably well with the known value of 400 ft. Thus, when high frequencies and long cable runs are involved, cable termination and impedance matching is very important. Note the improvement in constant

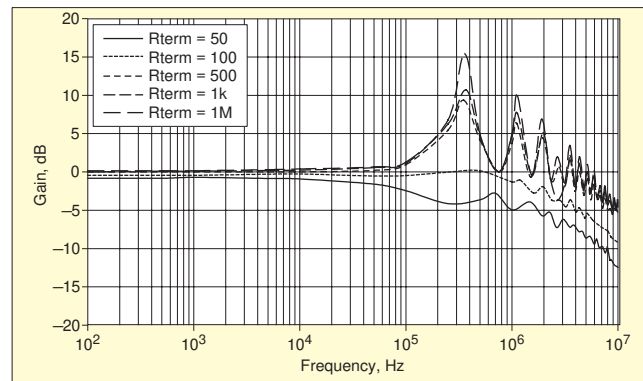


Figure 12. Response of Belden 22 AWG 4-conductor cable as a function of termination.

or 'flat' frequency response with the $R = 100 \Omega$ termination.

IEPE or ICP[®] sensors have an additional limitation associated with their high frequency response. For very long cable runs, one has to assure that there is adequate current to drive the cable capacitance. If the time varying current $i(t)$ supplied to the cable is $i(t) = I \sin 2\pi ft$, then at low frequencies:

$$v(t) = \frac{1}{C} \int i(t) dt = \frac{I}{2\pi f C} \cos(2\pi ft) \quad (6)$$

Here, C is the total cable capacitance. It can be seen that the magnitude of the measured voltage is inversely proportional to C , which is itself proportional to the length of the cable, so the measured voltage goes down with increasing cable length. The same inverse relationship holds for frequency. Conversely, the voltage is directly proportional to the current. The nomograph in Figure 13 plots these relationships.

To use this nomograph, let's take the previous example of the Belden #82418 cable with capacitance of 30 pf/ft. If we encountered 1,000 ft of cable back to a recording station, total capacitance would be 30,000 pF. If 100,000 Hz response and a maximum of 1 volt of signal level are required, the nomograph provides a value of $V/(i_c - 1)$ of 0.055. Note i_c is in milliamps and 1 is subtracted to account for the current required to power the ICP[®] electronics. Substituting, $1/(i_c - 1) = 0.055$ would result in a required supply current of 19.2 milliamps. 20 mA tends to be the maximum supply current for ICP circuits. If 5 volts maximum signal were required, and the maximum supply current were provided, $V/(i_c - 1) = 5/(20 - 1) = 0.263$. Entering the table where 0.263 on the ordinate intersects 30,000 pF yields an upper frequency limit of about 21,000 Hz. While proper cable termination (impedance matching) is likely not required for the 21,000-Hz signal, it definitely would be for the 100,000-Hz signal.

In some instances lower-capacitance cables can be substituted. For example, RG-62 type cable has one-half the capacitance-per-foot as does RG-58 type cable. However, it should always be remembered that when long cable lengths and high frequencies are involved, attention should be directed to both the inductance and capacitance of the cable. When possible, the cable frequency response should be checked by driving it through the same type ICP[®] circuit as will be used in the application.

Alternate Technologies

If all the preceding guidance in this article is adhered to, a valid signal representing the air-blast environment will be delivered for subsequent signal conditioning (e.g., digitizing and recording) and analysis. A final question to be addressed is whether there is an alternate technology to piezoelectric ICP[®] pressure transducers that should be considered for measuring the air-blast environment. The answer is yes; the alternate technology is MEMS ((M)icro(E)lectro(M)echanical (S)ystems)-based transducers.

Like ICP[®], silicon-based MEMS (piezoresistive) transducers are often used for air-blast pressure measurements. One reason is that mechanical strain is typically a desired response mea-

surement when structures are loaded by an air-blast. Therefore, strain-gage signal conditioning, i.e., differential amplifiers and power supplies, are usually already in place at the test facility, and these same signal conditioning devices can be applied directly to MEMS pressure transducers. This interoperability, not to mention the ease with which MEMS sensors can be statically calibrated, certainly encourages their utilization.

This section attempts to objectively compare strengths and weaknesses of MEMS and ICP® type pressure transducers focused only on their applicability to the air-blast environment. The analysis considers erroneous responses to the undesired stimuli that accompany air-blasts, which as previously noted, include as a minimum: thermal transients, light, acceleration/strain, and ionization products of the explosion. In addition, the transducer performance parameters of dynamic range, ruggedness/survivability, frequency response, and self-check are examined. We will deal with these issues one at a time in what this author considers their order of importance.

Thermal transients. Reference 8 discusses challenges encountered due to thermal-transient sensitivity of MEMS pressure transducers. Heat transfer by conduction, convection, and radiation results in the individual strain-elements of the pressure transducer's diaphragm encountering spatially distributed temperatures. These temperatures change with time and are different than that of their supporting structure. In addition, thermally induced distortion (e.g., bending) of the diaphragm can occur. The results of these combined effects are both a zero-shift and a change in sensitivity of the transducer. Figure 14 shows a pressure-time record acquired from a MEMS transducer in a contained explosive environment. This measurement was affected by thermal-transient stimuli.

Methods to mitigate thermal-transient response (as described in reference 8) include (1) a protective or shadowing screen over the diaphragm, (2) opaque grease in front of the diaphragm, and (3) the addition of an opaque material that adheres to the diaphragm such as black tape or RTV. Metallic coatings can also be added to the front of the diaphragm. All of these 'fixes' degrade the frequency response (discussed below) of the transducer to some extent as a byproduct of delaying the thermal transient.

References 9 and 10 describe recent advances using MEMS "silicon-on-insulator" (SOI) pressure transducer technology. This technology enables steady-state operation at temperatures to greater than 1000° F, while also enhancing transducer performance in thermal-transient environments.

The initial effect of transient temperature on quartz ICP® pressure transducers is to cause internal component dimensional changes (see Figure 5), which ultimately result in a partial release of the preload within the stack of quartz plates. The release of this preload results in an error in the pressure transducer output and a false indication of a positive pressure after the pressure event is over. A RTV coating is usually placed on the diaphragm of the transducer to provide a barrier to thermal transients. Coatings, placed on either MEMS or ICP® transducers, typically delay the thermal transient for no more than a few 10s of milliseconds.

Light. Reference 8 also discusses light-sensitivity of silicon transducers. This is of interest because light-intensity increases with proximity to the air-blast. Silicon-diaphragm pressure transducers absorb short-wavelength electromagnetic radiation in the wavelength range between 3,000 to 10,000 Å, most of which is in the visible spectrum. The temporary results are photoconduction as well as a photo diode effect in the junction isolation between the gages and the bulk material. Reference 8 concludes, "flash sensitivities of silicon diaphragms vary widely from unit to unit, and it is rather easy to obtain a full-scale output from a flash of light."

Again, since the publication of Reference 8, more recent SOI technology^{9,10}, used by select manufacturers, has greatly minimized transducer response attributable to light. By comparison, quartz ICP® technology has no sensitivity to light.

Frequency Response. MEMS pressure transducers typically

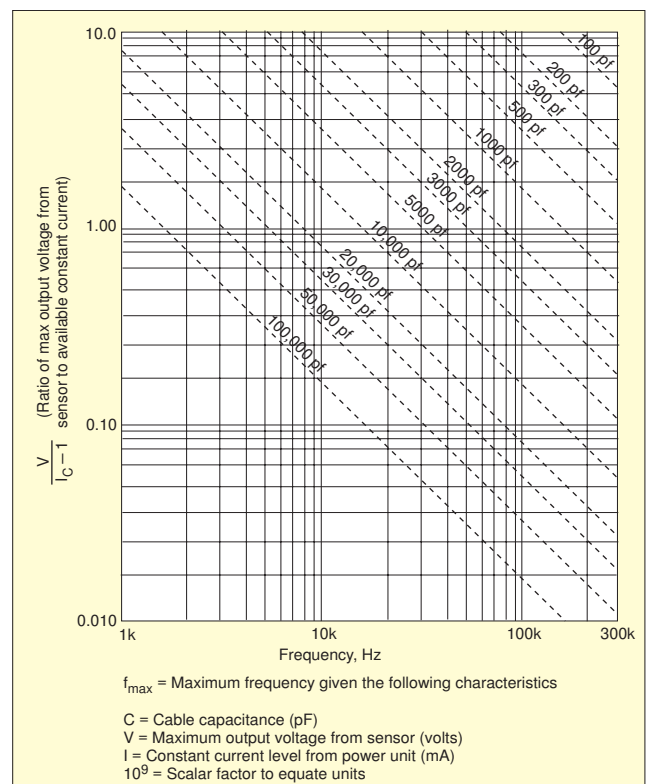


Figure 13. Nomograph showing effect of frequency and cable capacitance on ICP® signal output.

possess a maximum resonant frequency of 100 to 200 kHz at pressures under 100 psi extending to a 1 MHz resonance at 1,000 psi. Quartz ICP® transducers possess resonant frequencies of 300 to 400 kHz over this same pressure range. Frequency tailoring (mentioned previously in this article) extends the useable frequency response of quartz ICP® transducers. In addition, they do not require screens and are not influenced by the addition of coatings or RTVs to their diaphragms. MEMS transducers, in ranges less than 100 psi, typically find their frequency response degraded by the addition of thermal protective coatings to their diaphragms. This occurs due to the low density of silicon and the thinner diaphragms necessitated at the lower pressure-ranges. All quartz ICP® pressure transducers are extremely rigid, so as to be virtually unaffected by coatings.

Acceleration (Strain). As noted earlier, blast loading of the housing of a structure in which a pressure transducer is mounted creates motion of the structure and, additionally, induces mechanical strain into it. The lower profile of the MEMS silicon diaphragm assembly (< 0.015 in. thick), along with the low modulus/density ratio of silicon (approximately 1/3 that of steel), minimizes the acceleration response of MEMS pressure transducers. In addition, some MEMS SOI technology, analogous to ICP® technology, incorporates a 2nd transducer for acceleration compensation. When acceleration compensation is provided, the acceleration sensitivity of ICP® transducers is also very small; however, the larger, more complex structure of their sensing element (Figure 5) makes them more sensitive to strain coupling.

Ruggedness (Survivability). MEMS pressure transducers are specified with ranges to 30,000 psi, and, historically, with stated over-range capabilities of 2 or 3 times full-scale, without damage. Currently, select MEMS transducers⁹ are being fabricated with mechanical over-range stops to increase this capability. Quartz ICP® transducers are specified with ranges to 200,000 psi, with over-range capability in some instances of 200 times full-scale.

Dynamic range. MEMS pressure transducers typically provide an output signal of 100 to 200 millivolts without amplification. The basic piezoelectric sensing element in ICP® trans-

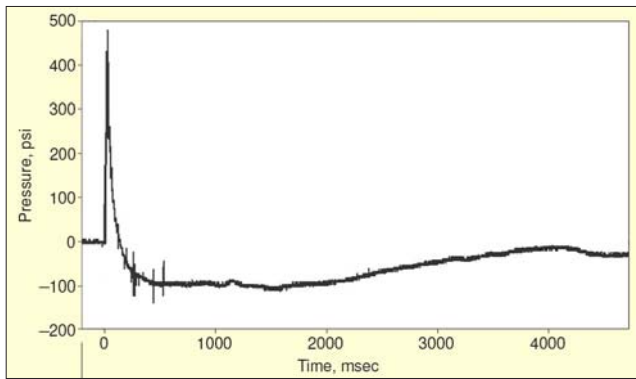


Figure 14. Erroneous blast pressure data (notice the -100 psig reading!).

ducers typically has a dynamic range of 100 to 120 dB. Quartz ICP® pressure transducers can readily provide a 5-volt full-scale output without amplification. Measuring a 100-psi blast-pressure wave with a 500-psi MEMS pressure transducer that has a 100 mV full-scale output would result in 20 mV of signal before amplification. The comparable measurement with a 500-psi ICP® transducer could result in 1000 mV of signal before amplification. This typical 50:1 signal ratio greatly reduces the number of ranges of ICP® transducers that have to be inventoried at a test facility.

Self-check. End-to-end checks of the integrity on the measurement system can be performed both with MEMS and ICP® transducers. With MEMS transducers one can shunt calibrate the system by paralleling a resistor across one arm of the bridge to produce a known voltage change. Calibration is somewhat of a misnomer, since the values of the transducer's bridge-resistors have some dependency on ambient temperature. Nevertheless, the signal indicates continuity and provides some measure of gain through the circuit, which is important information when long runs of cables are involved. The equivalent check for an ICP® transducer is the monitoring of the bias voltage associated with the MOSFET inside the transducer. This bias voltage serves as a continuity check.

Ionization products. MEMS and ICP® transducers can both be mounted with the transducer housing either grounded or ungrounded to a mounting plate. Both devices have low-impedance outputs, and various cable shielding options can be provided. Any relative advantage between the two technologies would have to be associated with the dynamic range of the ICP® transducer, which was credited above under "dynamic range."

Transducer cost has not been considered in the preceding discussion. The cost of lost test data is often priceless. If multiple channels of acceptable strain-gage signal conditioning are in place, the MEMS transducer is the most economical solution. If these existing and available channels are not in place, per channel costs favor the ICP® solution.

Table 1 recaps the preceding comparison. A (+) indicates the best or highest performance and a (X) lesser but still highly competitive performance. It should again be noted that the MEMS SOI pressure-transducer technology is currently emerging, and is only available from select manufacturers. The more

Table 1. Technical comparison of ICP® vs. MEMS transducers for an air-blast application.

Evaluation Parameter	ICP®	SOI	Silicon p-n
Thermal Transients	+	-	-
Light	+	x	-
Frequency Response	+	+	+
Acceleration (Strain)	x	+	x
Ruggedness (Survivability)	+	+	-
Dynamic Range	+	-	-
Self-Check	+	+	+
Ionization Products	+	+	+

(+) is best or highest performance
(x) is lesser but still highly competitive performance

significant observations include the ICP® sensors' greater tolerance to thermal-transient protection barriers (e.g., RTVs), as well as their much greater dynamic range, compared to the lower acceleration or strain response associated with MEMS SOI sensors. In many air-blast environments both MEMS and ICP® pressure transducers currently operate successfully. However, focusing only on this air-blast application, the ICP® pressure transducers are seen to have some advantage.

Conclusion


After briefly describing the air-blast environment, some of the historical challenges associated with its measurement were presented. Problems associated with interfacing a pressure transducer to the air-blast environment were next described, and analysis procedures were provided to calculate the effects of any transducer-mounting compromises. Tools for validation of data were then discussed, and methods to minimize any documented environment-induced noise, if present, were provided. The frequency limitations attributable to long cables runs used in air-blast testing were then described, and some computational tools were identified. Last, a comparison of different transducer technologies was performed.

Measurement of air-blast phenomena is a challenging task for the test engineer or technician. Hopefully this work will provide comprehensive guidance where a lack of it now exists.

References

- Walter, P. L., "Limitations and Corrections in Measuring Dynamic Characteristics of Structural Systems," Ph. D. Thesis, Arizona State University, pp. 140-141 and 205-208, Dec. 1978.
- Morse, P. M., *Vibration and Sound*, McGraw Hill, NY, ch. 22, pp. 221-235, 1948.
- Shock and Vibration Transducer Selection, Institute of Environmental Sciences and Technology, IEST RP-DTE011.1, Sec. 7.9, Oct. 2004.
- Stein, P. K., *The Unified Approach to the Engineering of Measurement Systems*, Stein Engineering Services, Phoenix, AZ, April 1992.
- Hilten, John, Vezzetti, Carol, Mayo-Wells, J. Franklin and Lederer, Paul, "Experimental Investigation of Means for Reducing the Response of Pressure Transducers to Thermal Transients," NBS Tech Note 961, January 1978.
- Matick, Richard L., "Transmission Lines for Digital and Communication Networks," IEEE Press, pp. 31-35, 1995.
- Belden CDT Inc., St. Louis, MO.
- Whittier, Robert M., "Reducing Transient Thermal Sensitivity of Silicon Diaphragm Pressure Transducers," Eleventh Transducer Workshop, Seattle, WA, available from: Secretariat Range Commander's Council, White Sands Missile Range, NM, pp. 292-301, June 2-4, 1981.
- Kurtz, A. D., Ainsworth, R. W., Thorpe, S. J. and Ned, A. A., "Further Work on Acceleration Insensitive Semiconductor Pressure Sensors for High Bandwidth Measurements on Rotating Turbine Blades," NASA 2003 Propulsion Measurement Sensor Development Workshop, Huntsville, AL, May 13-15, 2003.
- Kurtz, A. D., Ned, A. A. and Epstein, A. H., "Improved Ruggedized SOI Transducers Operational Above 600° C, Twenty-First Transducer Workshop, Lexington Park, MD, June 22-23, 2004.

A number of additional reference sources were consulted for this work. A few of the more valuable are noted below:

- Hilten, John S., Vezzetti, Carol F., Mayo-Wells, J. Franklin, and Lederer, Paul S., Experimental Investigation of Means for Reducing the Response of Pressure Transducers to Thermal Transients, NBS Technical Note 961, National Bureau of Standards, Washington, DC, January 1978.
- Hilten, John S., Vezzetti, Carol F., Mayo-Wells, J. Franklin, and Lederer, Paul S., A Test Method for Determining the Effect of Thermal Transients on Pressure-Transducer Response, NBS Technical Note 905, National Bureau of Standards, Washington, DC, January 1976.
- Sachs, Donald C., Cole, Eldine, Air Blast Measurement Technology, Report Defense Nuclear Agency #DNA 4115F, work performed by Kaman Sciences Corp. (K-76-38U(R), Colorado Springs, CO, September 1976.
- A Guide for the Dynamic Calibration of Pressure Transducers, ISA-37.16.01-2002, November 21, 2002. 

The author can be contacted at: p.walter@tcu.edu.